nature nanotechnology

LETTERS

PUBLISHED ONLINE: 2 MARCH 2014 | DOI: 10.1038/NNANO.2014.24

Three-dimensional manipulation with scanning near-field optical nanotweezers

J. Berthelot[1], S. S. Aćimović[1], M. L. Juan[2,3], M. P. Kreuzer[1], J. Renger[1] and R. Quidant[1,4]*

Recent advances in nanotechnologies have prompted the need for tools to accurately and non-invasively manipulate individual nano-objects[1]. Among the possible strategies, optical forces have been predicted to provide researchers with nano-optical tweezers capable of trapping a specimen and moving it in three dimensions[2–4]. In practice, however, the combination of weak optical forces and photothermal issues has thus far prevented their experimental realization. Here, we demonstrate the first three-dimensional optical manipulation of single 50 nm dielectric objects with near-field nanotweezers. The nano-optical trap is built by engineering a bowtie plasmonic aperture at the extremity of a tapered metal-coated optical fibre. Both the trapping operation and monitoring are performed through the optical fibre, making these nanotweezers totally autonomous and free of bulky optical elements. The achieved trapping performances allow for the trapped specimen to be moved over tens of micrometres over a period of several minutes with very low in-trap intensities. This non-invasive approach is foreseen to open new horizons in nanosciences by offering an unprecedented level of control of nanosized objects, including heat-sensitive biospecimens.

Building knowledge within the physical, chemical and biological sciences often requires fractionating complex and macroscopic mechanisms into simpler elementary ones on the nanometre scale. With this aim, researchers have put a great deal of effort into developing techniques for monitoring as well as controllably and non-invasively manipulating elementary units of matter down to the single atom/molecule level. Among these techniques, scanning probe microscopy has played a key role. Originally developed for imaging purposes, scanning tunnelling microscopy became a powerful way to manipulate individual atoms adsorbed at a surface[5]. Slightly later, the atomic force microscope followed a similar route and proved useful in picking up and moving slightly larger amounts of matter, typically with dimensions in the range of tens of nanometres, such as nanocrystals, nanoparticles or carbon nanotubes[6,7]. Interestingly, the optical version of scanning probe microscopy—near-field scanning optical microscopy (NSOM)[8,9]—was originally foreseen to also have nanomanipulation capability. In the 1990s, several theoretical studies predicted that the strong optical concentration produced at the tip of a sharply elongated metallic probe should create optical forces strong enough to stably trap dielectric objects with dimensions as small as a few nanometres[2–4,10–12]. Despite these predictions, this has never been reported experimentally, and has largely been prevented by photothermal effects[9] (L. Novotny, personal communication). Although this configuration offers strong optical gradients, the required level of local field intensity within the trap (larger than 1×10^{12} W m^{-2}), when accounting for the large intensity enhancement at the tip (for example, 3,000; ref. 2), is liable to damage either the specimen being trapped[13] or the tip itself[14–17]. When operating in liquid, absorption within the metal is also responsible for heat-induced fluid dynamics[18] or bubble formation[19], which may further jeopardize trapping. Here, we report on the first realization of optical trapping and manipulation of an individual nano-object at the extremity of an NSOM probe. Our nano-optical tweezers are formed at the extremity of a metal-coated tapered optical fibre patterned with a bowtie nano-aperture (BNA). We demonstrate stable optical trapping and accurate three-dimensional manipulation of a 50 nm polystyrene bead in water with local intensities within the trap as small as 1×10^{9} W m^{-2}. Such a level of intensity sits well below what would be required for conventional optical tweezers (typically from 1×10^{11} to 1×10^{12} W m^{-2}) and is compatible with heat-sensitive objects such as biospecimens.

Our present work capitalizes on the latest advances in near-field optical trapping[20–22] based on the so-called self-induced back-action (SIBA) mechanism, which dramatically relaxes the requirements on the local optical intensity and thus minimizes photothermal issues[23]. In SIBA trapping, the resonant optical nanostructure is designed such that its optical properties (resonance spectrum, local field distribution and intensity) significantly depend on the presence of the specimen. For a trapping laser slightly redshifted with respect to the central resonance wavelength of the nanostructure, the trap becomes stiffer when the specimen tends to escape as the result of the induced resonance shift. In other words, the trapped specimen plays an active role in the trapping mechanism in such a way that the required average local field intensity is weaker by orders of magnitude when compared with conventional trapping. Interestingly, the trap reconfiguration does not require any active monitoring of the specimen as it is automatically synchronized with its dynamics[24–26].

In practice, implementing SIBA trapping at the extremity of a tapered optical fibre first requires identifying a geometry of the SIBA trap that enables extended trapping times under low laser intensity, to prevent any photothermal damage at the fibre extremity. The typical damage threshold for such probes lies around 1×10^{10} W m^{-2} at the tip apex[17]. To remain below this threshold, we focused our attention on the so-called BNA design[27–29]. This geometry combines high collection cross-section and transmission with strong mode confinement under transversal polarization, making it a very good candidate for SIBA trapping. BNA supports two types of resonance: a Fabry–Pérot-like resonance that mainly depends on the film thickness, as well as two plasmonic resonances that depend on the geometry of the aperture[28]. Extensive three-dimensional numerical simulations based on COMSOL were performed to identify the most suitable design to achieve SIBA trapping at 1,064 nm on 100-nm-thick gold film covered with water. Parameters were chosen such that the transverse plasmonic mode (confined within the gap region) was slightly blue-detuned with respect to the trapping

[1]ICFO – Institut de Ciencies Fotoniques, Mediterranean Technology Park, 08860 Castelldefels (Barcelona), Spain, [2]Department of Physics & Astronomy, Macquarie University, Sydney, New South Wales 2109, Australia, [3]ARC Centre for Engineered Quantum Systems, Macquarie University, Sydney, New South Wales 2109, Australia, [4]ICREA – Institució Catalana de Recerca i Estudis Avançats, 08010 Barcelona, Spain. *e-mail: romain.quidant@icfo.es

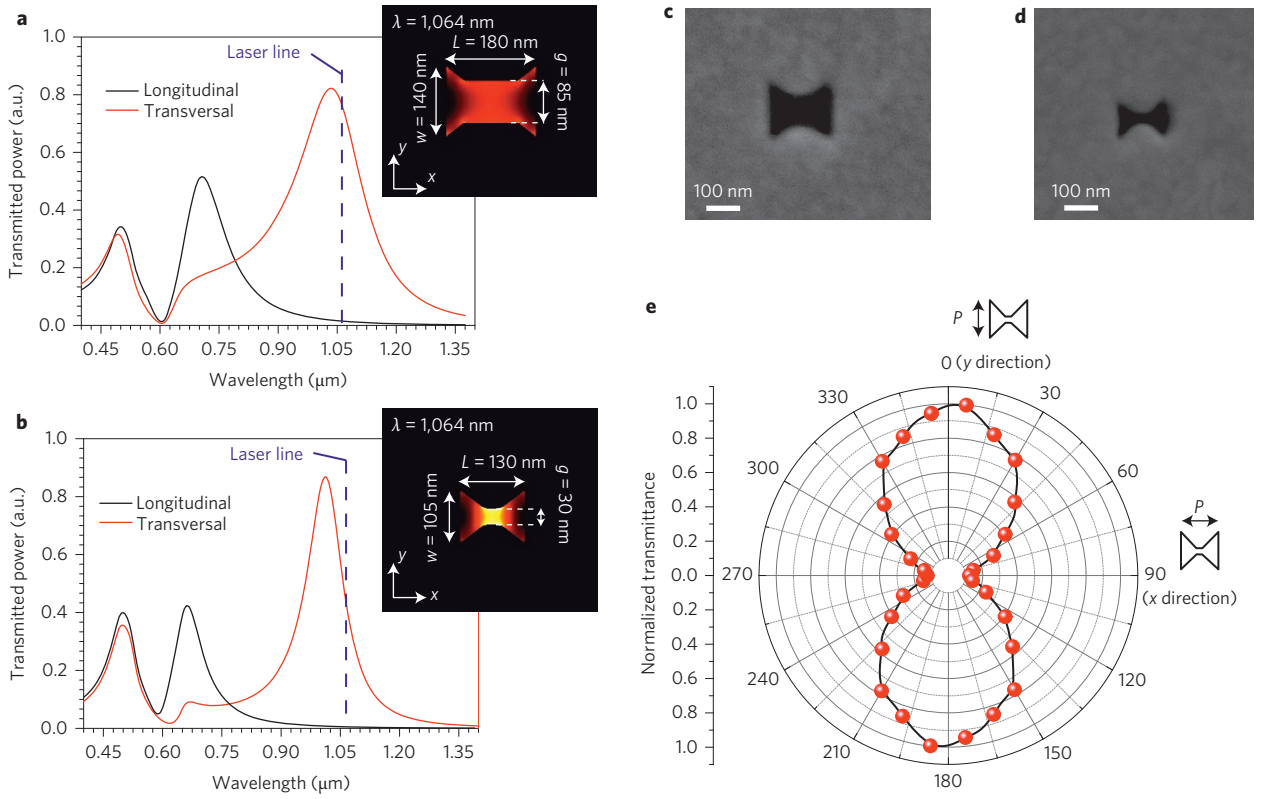

Figure 1 | Optical properties of BNAs. a–d, Calculated transmission spectra and near-field intensity maps (**a**,**b**) at 1,064 nm under transverse incident polarization for the two fabricated BNAs presented in the SEM images (**c**,**d**, respectively). **e**, Evolution of the experimental transmission at 1,064 nm as a function of incident polarization, *P*, for a 30 nm gap BNA.

wavelength. This condition was fulfilled for gap sizes between 30 nm and 85 nm by adjusting both the length and width of the antenna. Based on these simulations, BNAs were first fabricated in a planar geometry to evaluate and optimize their trapping performance. Figure 1c,d presents scanning electron microscopy (SEM) images of two fabricated apertures, with 85 nm and 30 nm gaps, respectively. The transmission spectra and near-field maps at 1,064 nm displayed in Fig. 1a,b were calculated from the experimental geometrical parameters extracted from Fig. 1c,d. As expected, the transverse mode confinement increases for decreasing gap sizes. In agreement with earlier studies, the enhancement of the local electric field intensity at the centre of the gap ranges from below 100 for the 30 nm gap to below 10 for the 85 nm gap[30]. To probe the transverse mode of the fabricated BNA, we also measured the evolution of the transmission through the aperture at 1,064 nm as a function of the incident polarization. In good agreement with the simulations, the polar transmission plot of a 30 nm gap BNA (Fig. 1e) features a maximum when the incident electric field aligns across the gap (*y* axis).

Figure 2 illustrates the trapping performance of a BNA with a 30 nm gap. The aperture was exposed to a diluted aqueous solution (0.05% wt/vol) of 20 nm fluorescent polystyrene beads (absorption at 532 nm/emission at 612 nm) containing a 1% concentration of SDS solution to prevent aggregation. Figure 2a provides a schematic of the experimental configuration. The 1,064 nm trapping laser was linearly polarized along the *y* axis before being slightly focused (from the water side) onto the BNA with a ×40 objective lens (0.65 NA), producing an illumination spot of ~2 μm. A 532 nm laser was added to the same optical path to simultaneously excite the bead fluorescence. The transmission through the BNA at 1,064 nm and the fluorescence from the bead were monitored over time by two independent photodetectors (see Methods). A typical portion of the experimental time traces, demonstrating optical trapping of a single 20 nm bead for an irradiance of 1.27×10^9 W m^{-2}, is presented in Fig. 2b. Trapping was monitored by the increase of the transmission signal resulting from the local increment of refractive index induced by the presence of the particle[23–25]. Statistical analysis of the data enabled the identification of two transmission levels corresponding to an empty trap and trapping of a single bead. This interpretation was further confirmed by the fluorescence time trace, which displays an increase exactly coinciding with the increased level of transmission. Trapping times longer than 30 min were achieved under these illumination conditions. We also systematically checked that the trapped nanoparticle did not stick to the antenna and was released when switching off the trapping laser (Supplementary Fig. 1). To test the robustness of SIBA trapping with the BNA geometry, we also performed additional experiments using larger gaps of 85 nm. Despite the weaker confinement of the mode (translating into a weaker effect of the trapped specimen on the BNA resonance), both 50 nm and 20 nm polystyrene beads were successfully trapped over several minutes using incident powers between 2 and 5 mW (0.63×10^9 W m^{-2} and 1.59×10^9 W m^{-2}), respectively.

At this stage, optimized in-plane BNA trapping was implemented at the extremity of a scanning tapered metallized optical fibre to achieve nano-optical tweezers capable of manipulating the trapped specimen in three dimensions. The fabrication process used to prepare the tapered fibres was adapted from ref. 17. Briefly, a single-mode optical fibre was tapered by laser pulling and coated with 200 nm aluminium to prevent light leakage through the sides of the cone. Focused ion beam (FIB) milling was used to cut the tip extremity to obtain a flat facet, which was subsequently metallized with 100 nm of gold. Finally, the BNA was milled by FIB at the centre of the 1-μm-diameter gold platform. An example of a fabricated tweezers is shown in the SEM image in Fig. 3a. It is worth mentioning that, with the FIB we used, fabrication of the 30-nm-gap BNAs required exposure

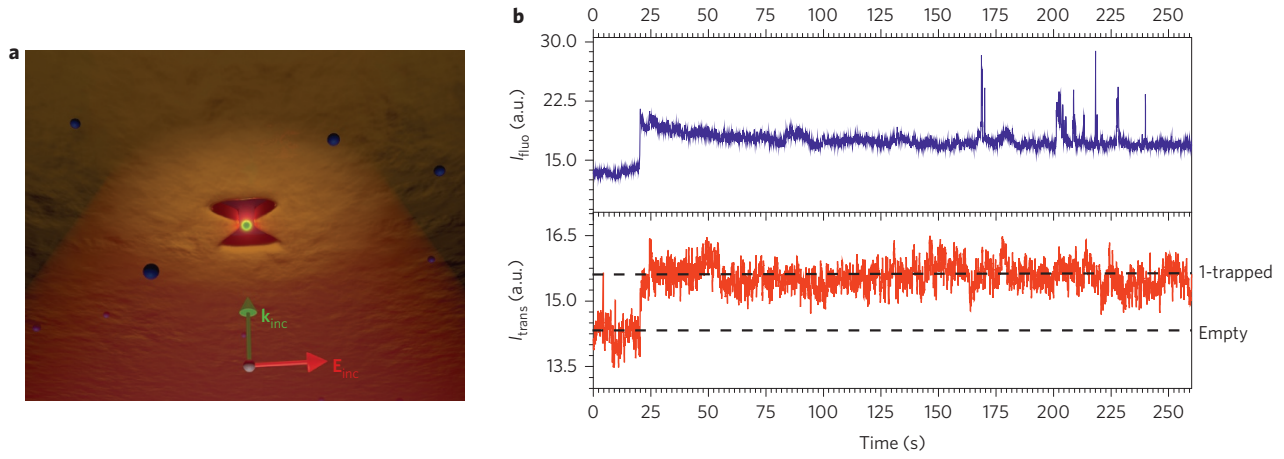

Figure 2 | SIBA trapping of a single 20 nm polystyrene bead in a planar geometry. a, Schematic of experimental configuration. A 30-nm-gap BNA is illuminated from the water side with a 1,064 nm laser beam, linearly polarized along the *y* axis, and slightly focused with a ×40 (0.65 NA) objective lens. **b**, Experimental time traces showing transmission through the BNA at 1,064 nm (red curve) and fluorescence from the trapped bead (blue curve). The increase in both transmission and fluorescence corresponds to the trapping of a single 20 nm polystyrene bead.

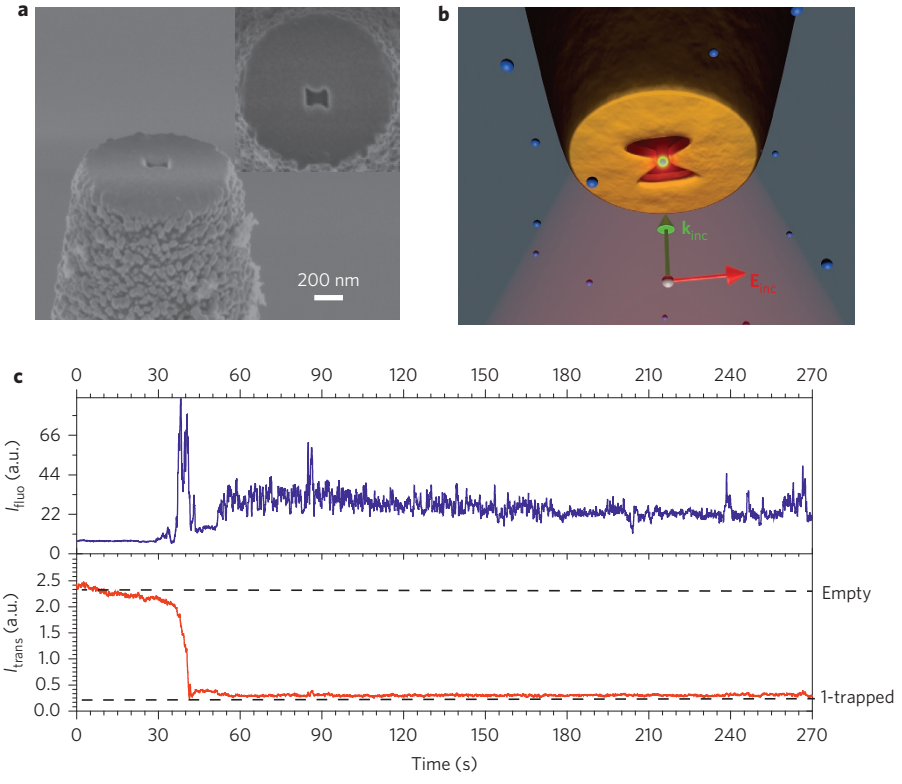

Figure 3 | SIBA trapping at the extremity of a patterned tapered fibre under external illumination. a, SEM image of an 85-nm-gap BNA patterned at the extremity of a tapered optical fibre. **b**, Schematic of the experimental configuration: the antenna is illuminated from the water side with a 1,064 nm laser beam focused through a ×40 (0.65 NA) objective. The incident polarization is aligned along the BNA gap to excite its transverse mode. **c**, Portion of the time traces of the 1,064 nm signal detected by the fibre (red) and the fluorescence from the bead (blue) detected by the objective lens. A 50 nm polystyrene bead enters the aperture area around $t = 35$ s and is stably trapped after $t = 40$ s.

parameters that were not compatible with fully preserving the integrity of the fibre output facet. For this reason, in the following, we limit ourselves to gaps of 85 nm. For the trapping experiments, the fabricated fibres were mounted on a three-dimensional piezoelectric scanner and introduced into a modified fluidic chamber (see Methods) containing a solution of 50 nm polystyrene beads (same parameters as in the in-plane experiments). We tested two trapping schemes based on different illumination conditions; either through an objective lens or through the fibre itself.

In the first configuration, schematically presented in Fig. 3b, the 1,064 nm laser was focused through the ×40 objective (0.65 NA) and centred on the BNA. The transmitted light was collected through the fibre and sent to a silicon photodetector. The fluorescence from the bead was collected back through the same objective lens before being focused on an avalanche photodiode using a confocal detection. Figure 3c presents a portion of typical time traces, demonstrating the trapping of a single 50 nm bead using an incident power of 4 mW (1.27×10^9 W m^{-2}). In this

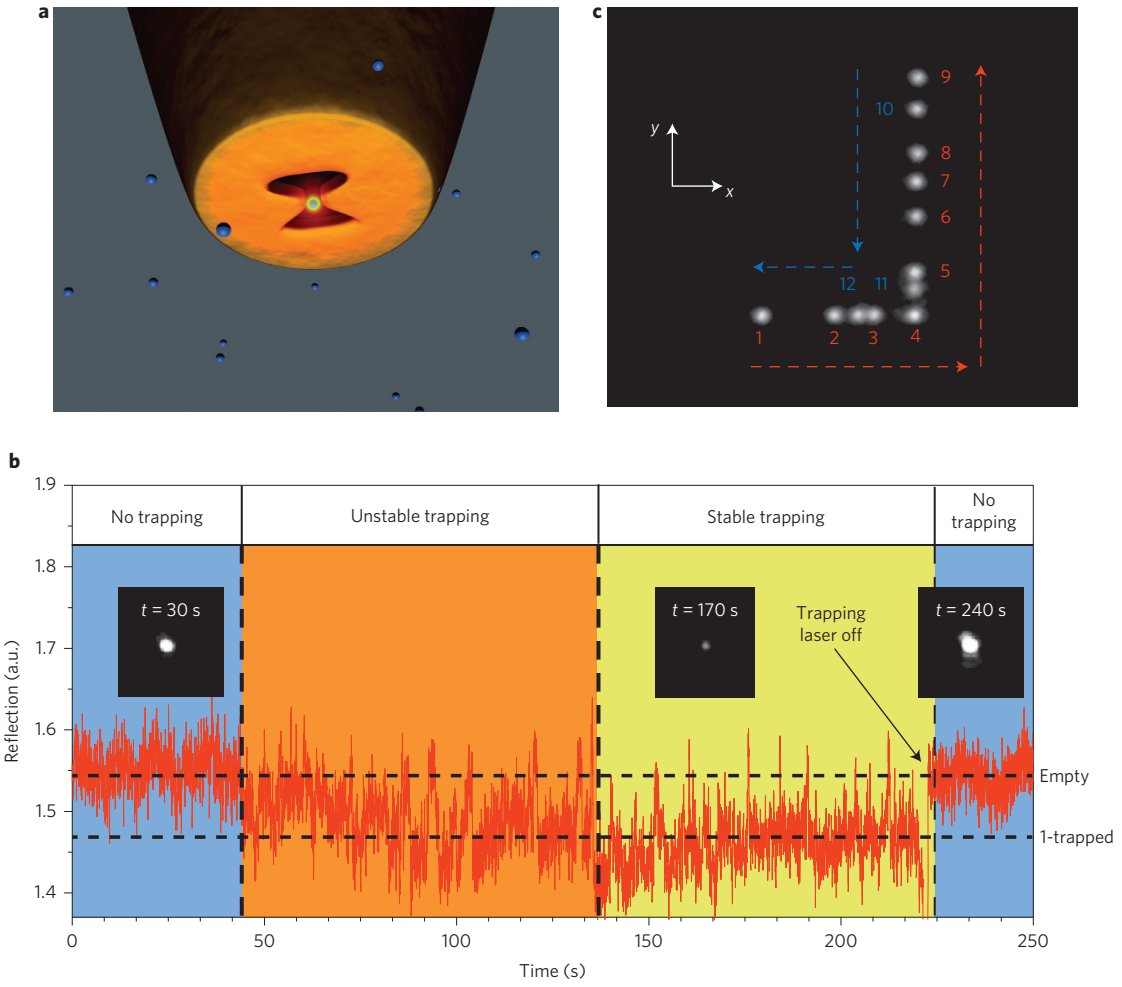

Figure 4 | Three-dimensional manipulation of a single 50 nm polystyrene bead. a, Schematic of experimental configuration. The 1,064 nm trapping laser is directly coupled into the fibre to excite the transverse mode of the BNA. **b**, Experimental time trace of the reflected 1,064 nm signal showing trapping of a single 50 nm polystyrene bead. Insets: Optical images of the fibre transmission spot at different times. **c**, Composite image reproducing the displacement of the trapped object. This displacement takes place during the time period $t = 180$–210 s of time trace **b**. Numbers 1–12 represent the successive steps of the tip movement. See also Supplementary Movie.

configuration, unlike what was observed in the planar sample, the trapping event is associated with a decrease in the transmitted signal. This decrease is attributed to the detection through the fibre. Because of its subwavelength size, the nanobead scatters light over a wide range of **k**-vectors, thus decreasing the amount of light coupled into the fibre mode. This interpretation is consistent with the simultaneous increase in the fluorescence signal, confirming the presence of the nanobead within the BNA. As for the in-plane configuration, we verified that the particle was released when switching off the trapping laser (Supplementary Fig. 2). Although stable trapping was achieved for more than 3 min, this configuration has some issues. First, the trap position is fixed and does not take advantage of the tip mobility. Second, because the tapered fibre and the collection objective are physically independent, vibrations and small drifts in their relative position produce additional noise, making monitoring and analysis of the trapping events more difficult.

To overcome these issues, we switched to the second configuration where both illumination and collection are performed through the fibre. For this purpose we implemented a (90/10) fibre coupler combined with a polarization-maintaining (PM) fibre designed for 1,064 nm. Polarization of the incoming 1,064 nm laser (10% arm) was controlled at the entrance of the PM fibre and set to maximize the transmission through the BNA. The 1,064 nm light reflected by the tapered end face of the fibre was then collected by the 90% arm and focused on a silicon photodetector. A schematic of the experimental configuration is provided in Fig. 4a. With this configuration, both excitation and detection can be made using only the fibre. Additionally, the transmission collected by a $\times 40$ objective (0.65 NA) was imaged on a charge-coupled device (CCD) camera. A typical time trace of the reflected signal through the fibre is plotted in Fig. 4b. To estimate the incident intensity reaching the BNA plane, power measurements were systematically performed on aluminized tapered fibres before deposition of the gold layer. Powers ranging from 350 to 675 μW, depending on the taper angle, were measured at the output of the fibre end facet. The corresponding local intensities ranging from 4×10^9 W m^{-2} to 8×10^9 W m^{-2} (accounting for the tenfold theoretical intensity enhancement within the antenna gap) sit below the fibre damage threshold[17]. Similar to the previous trapping experiment, we identify in Fig. 4b two different levels in the reflected 1,064 nm signal, corresponding to the empty trap (higher level) and trapping of a single nanobead (lower level) (Supplementary Fig. 3). Trapping also corresponds to a decrease in the intensity of the transmitted signal recorded by the CCD camera. A closer look at the time trace of Fig. 4b enables us to distinguish three successive regimes: no trapping (blue area), unstable trapping (orange area) and stable trapping (yellow area). During the unstable trapping regime

(40 s $< t <$ 135 s), the nanobead moves within the BNA without reaching the equilibrium position in the gap region, leading to large fluctuations in both the reflected and transmitted signals. As this behaviour was not observed in the previous configuration, this suggests that the illumination through the objective helps to push the particle towards the equilibrium position. Around $t = 140$ s, both signals become more steady, with the beginning of a stable trapping regime. Once the stable trapping regime was reached, the fibre was raster-scanned in all three spatial directions (see Supplementary Movie). The scan trajectory is shown in Fig. 4c, in which we have superimposed different CCD images from different time instances. The displacement of the tip was ~15 μm in the plane (x–y) and ~5 μm in the z direction. Finally, we verified that the trapped nanobead did not stick to the BNA and could be released by blocking the trapping beam ($t = 215$ s).

In conclusion, we have developed the first nano-optical tweezers capable of three-dimensionally manipulating (with nanometre accuracy) sub-100-nm dielectric objects over large ranges. We envision this approach could open new opportunities in various fields of science. In the context of biology it may enable non-invasive manipulation of individual nano-units such as viruses or large proteins[31]. It may also benefit the field of materials science, with the possibility of isolating, manipulating and controllably arranging solid-state nano-objects such as nanocrystals.

Methods

Microfluidic chamber for fibre trapping. The fluidic chamber used for fibre trapping was made of polydimethylsiloxane (PDMS) and a curing agent (5:1 by volume). With this mixture we obtained a PDMS piece measuring 20 mm × 20 mm × 5 mm. The chamber volume was made by removing the inner part of this piece. A thin membrane made with a solution of PDMS/curing agent (20:1 by volume) was fixed on top to prevent liquid evaporation. A hole (2 mm in diameter) was created in the centre of the membrane, allowing the introduction of the structured fibre. The complete PDMS piece was chemically bonded (12 h at 80 °C in the oven) to a 170-μm-thick glass substrate. The chamber was then completely filled with the solution of nanobeads via an inlet.

Optical set-up. We used a homemade inverted microscope. The trapping laser was a continuous-wave 1,064 nm Nd-YAG laser, the beam of which was extended and collimated to an 8-mm-diameter beam before being focused on the sample plane with a dry ×40 microscope objective (0.65 NA). A visible diode laser at 532 nm was focused on the sample at the same position as the trapping laser to excite bead fluorescence, and the same objective was used for fluorescence excitation and collection. The collected fluorescence was separated from the trapping laser beam with a dichroic mirror (reflecting 532 nm and 1,064 nm, and transmitting otherwise) and bandpass filter (580 nm to 640 nm), and then focused onto an avalanche photodiode in a confocal detection mode. The transmission of the trapping laser through the BNA was collected with a ×10 dry objective (0.22 NA) and sent to a photodiode. The polarization of the 1,064 nm laser was controlled by a polarizer and a half-wave plate. The incoming laser power was limited to a maximum of 10 mW in the sample plane. The acquisition signals were obtained using a Labview program at a sampling rate of 1 kHz.

Received 8 November 2013; accepted 20 January 2014; published online 2 March 2014

References

1. Maragò, O. M., Jones, P. H., Gucciardi, P. G., Volpe, G. & Ferrari, A. C. Optical trapping and manipulation of nanostructures. *Nature Nanotech.* **8,** 807–819 (2013).
2. Novotny, L., Bian, R. & Xie, X. Theory of nanometric optical tweezers. *Phys. Rev. Lett.* **79,** 645–648 (1997).
3. Martin, O. J. F. & Girard, C. Controlling and tuning strong optical field gradients at a local probe microscope tip apex. *Appl. Phys. Lett.* **70,** 705–707 (1997).
4. Chaumet, P., Rahmani, A. & Nieto-Vesperinas, M. Optical trapping and manipulation of nano-objects with an apertureless probe. *Phys. Rev. Lett.* **88,** 123601 (2002).
5. Hla, S-W. Scanning tunneling microscopy single atom/molecule manipulation and its application to nanoscience and technology. *J. Vac. Sci. Technol. B* **23,** 1351–1360 (2005).
6. Kim, S., Shafiei, F., Ratchford, D. & Li, X. Controlled AFM manipulation of small nanoparticles and assembly of hybrid nanostructures. *Nanotechnology* **22,** 115301 (2011).
7. Decossas, S. *et al.* Nanomanipulation by atomic force microscopy of carbon nanotubes on a nanostructured surface. *Surf. Sci.* **543,** 57–62 (2003).
8. Betzig, E., Lewis, A., Harootunian, A., Isaacson, M. & Kratschmer, E. Near field scanning optical microscopy (NSOM): development and biophysical applications. *Biophys. J.* **49,** 269–279 (1986).
9. Hecht, B. *et al.* Scanning near-field optical microscopy with aperture probes: fundamentals and applications. *J. Chem. Phys.* **112,** 7761–7774 (2000).
10. H'dhili, F., Bachelot, R., Lerondel, G., Barchiesi, D. & Royer, R. Near-field optics: direct observation of the field enhancement below an apertureless probe using a photosensitive polymer. *Appl. Phys. Lett.* **79,** 4019–4021 (2001).
11. Chaumet, P., Rahmani, A. & Nieto-Vesperinas, M. Photonic force spectroscopy on metallic and absorbing nanoparticles. *Phys. Rev. B* **71,** 045425 (2005).
12. Okamoto, K. & Kawata, S. Radiation force exerted on subwavelength particles near a nanoaperture. *Phys. Rev. Lett.* **83,** 4534–4537 (1999).
13. Ashkin, A., Dziedzic, J., Bjorkholm, J. & Chu, S. Observation of a single-beam gradient-force optical trap for dielectric particles in air. *Opt. Lett.* **22,** 816–818 (1986).
14. Xin, H., Xu, R. & Li, B. Optical trapping, driving, and arrangement of particles using a tapered fibre probe. *Sci. Rep.* **2,** 818 (2012).
15. Liberale, C. *et al.* Miniaturized all-fibre probe for three-dimensional optical trapping and manipulation. *Nature Photon.* **1,** 723–727 (2007).
16. Liu, Z., Guo, C., Yang, J. & Yuan, L. Tapered fiber optical tweezers for microscopic particle trapping: fabrication and application. *Opt. Express* **14,** 12510–12516 (2006).
17. Neumann, L. *et al.* Extraordinary optical transmission brightens near-field fiber probe. *Nano Lett.* **11,** 355–360 (2011).
18. Donner, J., Baffou, G., McCloskey, D. & Quidant, R. Plasmon-assisted optofluidics. *ACS Nano* **5,** 5457–5462 (2011).
19. Fang, Z. *et al.* Evolution of light-induced vapor generation at a liquid-immersed metallic nanoparticle. *Nano Lett.* **13,** 1736–1742 (2013).
20. Righini, M. *et al.* Nano-optical trapping of Rayleigh particles and *Escherichia coli* bacteria with resonant optical antennas. *Nano Lett.* **9,** 3387–3391 (2009).
21. Grigorenko, A. N., Roberts, N. W., Dickinson, M. R. & Zhang, Y. Nanometric optical tweezers based on nanostructured substrates. *Nature Photon.* **2,** 365–370 (2008).
22. Juan, M. L., Righini, M. & Quidant, R. Plasmon nano-optical tweezers. *Nature Photon.* **5,** 349–356 (2011).
23. Juan, M. L., Gordon, R., Pang, Y., Eftekhari, F. & Quidant, R. Self-induced back-action optical trapping of dielectric nanoparticles. *Nature Phys.* **5,** 915–919 (2009).
24. Pang, Y. & Gordon, R. Optical trapping of 12 nm dielectric spheres using double-nanoholes in a gold film. *Nano Lett.* **11,** 3763–3767 (2011).
25. Chen, C. *et al.* Enhanced optical trapping and arrangement of nano-objects in a plasmonic nanocavity. *Nano Lett.* **12,** 125–132 (2012).
26. Descharmes, N., Dharanipathy, U. P., Diao, Z., Tonin, M. & Houdré, R. Observation of backaction and self-induced trapping in a planar hollow photonic crystal cavity. *Phys. Rev. Lett.* **110,** 123601 (2013).
27. Kinzel, E. C. & Xu, X. Extraordinary infrared transmission through a periodic bowtie aperture array. *Opt. Lett.* **35,** 992–994 (2010).
28. Guo, H. *et al.* Optical resonances of bowtie slot antennas and their geometry and material dependence. *Opt. Express* **16,** 7756–7766 (2008).
29. Jin, E. X. & Xu, X. Plasmonic effects in near-field optical transmission enhancement through a single bowtie-shaped aperture. *Appl. Phys. B* **84,** 3–9 (2006).
30. Mivelle, M., van Zanten, T. S., Neumann, L., van Hulst, N. F. & Garcia-Parajo, M. F. Ultrabright bowtie nanoaperture antenna probes studied by single molecule fluorescence. *Nano Lett.* **12,** 5972–5978 (2012).
31. Pang, Y. & Gordon, R. Optical trapping of a single protein. *Nano Lett.* **12,** 402–406 (2012).

Acknowledgements

This work was partially supported by the Spanish Ministry of Sciences (grants FIS2010–14834), the European Community's Seventh Framework Programme (grant ERC-Plasmolight; no. 259196) and Fundació privada CELLEX. The authors thank M. Mivelle and M. García-Parajo for discussions.

Author contributions

J.B., M.L.J. and R.Q. conceived and designed the experiment. J.B. performed the experiments and analysed the data. S.S.A. performed the numerical simulations. All authors discussed the results and wrote the manuscript.

Additional information

Supplementary information is available in the online version of the paper. Reprints and permissions information is available online at www.nature.com/reprints. Correspondence and requests for materials should be addressed to R.Q.

Competing financial interests

The authors declare no competing financial interests.